Comprehensive Approach for Optimal Diesel Engine Downsizing Combining Thermodynamics and Design Assistance System

V. Dolecek[1], J. Macek[1], A. Barak[1], O. Vitek[1], S. Bogomolov[1], A. Mikulec[1]

1: Czech Technical University in Prague, Technicka 4, Prague 6, 166 07, Czech Republic

Abstract: The current uncertainty in the best solution of future vehicle powertrains calls for the advanced method for the fast assessment of impact of intended innovations.

Thermodynamic parameters of downsized and/or downspeeded engine for very high bmep (up to 35 bar) influence engine mass and overall dimension of engine concept design and configuration and they cannot be estimated by scaling of designs already available.

The thermodynamic substance of the cycle may be simulated without too detailed assumption of the certain partial phenomena realization (e.g., burning pattern), if sensitivity analysis is done before. Simulation methods coupling different level of method depth, as 1-D methods with in-house codes for engine mechanical efficiency assessment and preliminary design of boosting devices (a virtual compressor and a turbine), have been used together with optimization codes based on genetic algorithms. Simultaneously, the impacts of optimum cycle on components dimensions, mass and inertia force loads were estimated since the results were systematically stored and analyzed in Design Assistance System DASY, developed by the authors for purposes of early-stage conceptual design.

Operation fuel consumption has been simulated using updated powertrain and vehicle mass data. NEDC and ARTEMIS tests were applied. The final assessment of downsized engine feasibility has been based on it.

Keywords: downsizing, downspeeding, 1-D modelling, engine thermodynamic optimization, driving cycle simulation

1. Introduction

Downsizing is often referred to as a way for increasing engine brake efficiency (due to reduction of relative thermal and mechanical losses) and improving road fuel consumption due to higher load of an engine in operation. Simultaneously, engine size and mass are reduced, which is accompanied by vehicle driving resistance decrease. On the other hand, much higher peak pressures occur, which has to be taken into account in dimensioning engine components. More robust components increase relatively the engine mass and cost, impacting mechanical losses in a cranktrain, as well. In the case of any of apparently low-temperature combustion systems, efficient boost pressure charging of cylinders is required due to mixture dilution.

Downsizing may be accompanied by downspeeding, reflected in lower cycle frequency (speed in rpm). Despite all efforts, the real limits of design have not yet been found – [1] and [2]. Recently, the same issues for truck and passenger car engines were addressed – e.g., [3] and [4]. The optimum solution depends on the total effects of new design on a new product. Moreover, the described issues should be optimized for real driving conditions, hopefully reflected in test procedures, considering both fuel efficiency together with CO2 and other GHG emissions fulfilling future pollution standards.

The clear way to totally optimum downsized engine has been found in [15] and [16]. The main issue consisting in difficult early stage decision of a new engine design concept considering future (yet not designed) vehicle performance has been solved by the original Design Assistance System DASY.

The tools for doing this uneasy task and results of fully optimized downsized engine are being intensively developed, which is, e.g., described in the current paper as a continuation of authors' previous studies – [5,] [8],[15] and [16]. These first attempts to optimize both efficiency and engine mass accompanied by main design parameters estimation at different loads/speeds are being now followed by powertrain and vehicle design changes including powertrain control systems.

For this preliminary study, a really existing four cylinder, diesel engine of 1.65 dm^3 displacement volume has been used. Unlike in other published studies, the optimization of brake specific fuel consumption was done using minimal number of constraints to find the total optimum. The efficient exhaust gas aftertreatment system (like SCR) is assumed, which sets almost no limits to thermodynamic optimization. The low-temperature combustion modes have been implicitly taken into account – [15]. The potential of alternative combustion patterns has been tested, as well – [16].

The goal of those efforts has been finding the optimum envelope of possibilities limiting any future real solution. The partially optimized realizable designs with reduced flexibility of engine controlled parameters will fit into this envelope. The assessment of the distance of real design to this total optimum will help in deciding what change will be worthwhile for the next design improvement.

Simultaneously, the holistic approach may take all significant vehicle and powertrain features into consideration as early as during concept stage of development. A further step on this way is described in the current contribution. After the steady operation cycles have been optimized the assessment of real operation on the road fuel consumption is tested here

together with the prediction of engine unsteady operation.

2. Main Steps of New Approach to ICE Optimization

The authors used the previous experience and tools based on in-house development (knowledge database DASY [5], in connection with specific codes, e.g., for mechanical loss estimation – [9], turbocharger parameters definition – [10], crankshaft safety factors assessment – [8], etc.) together with commercial software products (e.g., GT Suite).

The reference diesel engine of 1.65 dm^3 displacement with conservative dimensions (bore of 80 mm, stroke of 82 mm) and bmep of 25 bar in the range of 1 000 – 4 000 rpm was used as an initial prototype. The initial parameters, including pressure losses, discharge coefficients and mechanical efficiency, are based on real engine tests.

Brake mean effective pressure (bmep) has been increased up to 35 bar during the current optimization, keeping the power at different speeds equal to the initial diesel engine. The displacement of all new downsized engines was thus reduced. The stroke was either unchanged, keeping mean piston speed without change (no downspeeding neither in rpm nor in mean piston speed), or it was a free parameter to be optimized in certain cases (distinguished in the explanations below from the former approach as optimized mean piston speed c_s). The latter case leads both to downspeeding or overspeeding in terms of mean piston speed. Optimization of stroke was performed for any operation point in an independent way, i.e., not taking engine optimum design for other speeds into account. The sensitivity to this practically hardly applicable measure is commented below.

No other constraints were limited during thermodynamic optimization, as, e.g., peak pressure as well as piston surface temperature, turbine inlet temperature or valve temperatures, which has created novel approach, yielding unprejudiced view on the total optimum of efficiency of the optimized engine.

Other novelty of this approach has been a direct coupling of thermodynamic optimum results to engine design changes, reflected by engine dimensions and to mechanical loss estimation of more detailed cranktrain model with friction described by Stribeck curves – [9]. The main components were preliminarily designed, taking changes of bore, stroke and peak pressure into account, e.g., [8].

A scheme of data flows with future amendments up to vehicle data is presented in Figure 16 (see Appendix). In the current paper, the parameters up to cylinder block and cylinder head mass were predicted as a feedback to thermodynamic optimization together mass and moments of inertia for engine dynamics prediction.

3. Engine Efficiency Optimization

3.1 Constraints and basic boundary conditions

The thermodynamic optimization was based on calibrated 1-D model of diesel engine in GT-Power – [15]. The original 4-cylinder engine has bore/stroke 80/82 mm.

All initial dimensions and loss coefficients were taken from this real engine for both aerodynamic and mechanical losses. The combustion, represented by semi-predictive three-term ROHR Vibe function with the main phase 0-95% duration dependent on air excess and speed, was used, taking into account changes relative to reference burn duration at reference air excess and engine speed – [13] or [14]. The rate of heat release was optimized, but considering its position and duration only, since the shape is not very important in a wide range of shape changes – e.g., [1]. Two optimized variants of reference length of combustion 20 and 35 degrees CA were applied as reference cases and recalculated by Woschni combustion duration dependence on speed (duration proportional to the square root of engine speed) and air excess (duration reversely proportional to the 0.6 power of air excess).

A simplified FEM model of cooled walls was used for fire surface temperature assessment at all components in contact with gas in a cylinder. Woschni heat transfer formula was applied, up to now without correcting multipliers.

Turbocharger maps were created for a virtual compressor (not limited by surging or choking but using reasonable compressor efficiency dependent on compressor pressure ratio) and turbine map derived from original one by multiplier of mass flow rate which substituted the VNT, again with feasible averaged rated efficiency – [10]. They are relevant for downsized engine. The turbine efficiency reached at the engine takes into account the pulsations in exhaust system. Turbine diameter was optimized considering the optimum usage of turbine map. This approach is very important for finding limits of ultimately achievable brake efficiency including pumping work of the engine. The specific matching of a compressor and a turbine has to be done later but the limits for comparison to ideal case have been already set. Moment of inertia was estimated for this virtual single stage turbocharger. During the further research, the model will be replaced by two/stage turbocharging group.

The whole turbocharging group was replaced by a virtual turbocharger with multipliers of size and speed. The turbocharger was adjusted by multipliers to required flow rate and for demanded boost pressure at any operation point. There were two optimized variants of the total two stage turbocharger group efficiency of 50% and 60% (defined from isentropic enthalpy difference at compressor and turbine sides, including compressor side intercooling and all pressure losses). The size of valves and ports and dimensions of combustion chamber in piston were proportionally modified to engine bore.

Mixture strength (i.e., boost pressure), compression ratio up to 18 and all currently variable engine data (combustion timing, valve timing and a virtual turbocharger matching, surrogating two-stage turbocharger group) have been optimized as well, in dependence on engine speed and brake mean effective pressure at speed-appropriate constant power.

The optimized engine features fixed torque output defined by 25 bar of bmep in the whole engine speed range from 1000 to 4000 rpm. Downsized versions were made by reducing engine displacement volume to keep the output parameters at the same level by increasing engine specific outputs. The engine was downsized in two steps with 30 and 35 bar of bmep using two approaches to piston stroke. In the first one, the mean piston speed was kept constant and reduced was only engine bore. In the second one, the bore/stroke ratio was variable in a wide range.

The genetic optimization algorithm was used to search for the optimum settings of parameters listed above. The genetic algorithm was applied with 72 designs in one generation and 30 generations. The bsfc was minimized to find the highest possible value of all efficiencies.

4. Results of Steady Cycle Optimization at WOT

The comprehensive list of steady operation results has been published in [15] and [16]. As an example, the fuel consumption for several optimized variants at 1 000 and 4 000 rpm is displayed in Figure 1 and Figure 2. The positive influence of higher specific load can be observed if engine speed is high enough. At lower speeds, the stagnation of bsfc at speeds lower than 2 000 rpm can be found. The significance of high turbocharger total efficiency is obvious. Additional reduction of fuel consumption can be achieved by optimization of bore/stroke ratio for given operation conditions. A little surprisingly, the peak pressure was kept limited to reasonable and achievable values, although it was unlimited during optimization. In addition, the advantage of very short combustion duration is not prominent, which limits the contribution of HCCI-like combustion. In all cases, reasonably short combustion (reference duration of 35°CA) is better than extremely short one.

Too high air-to-fuel ratio requires very high boost pressure but yields only low exhaust gas enthalpy, which causes high pumping work. Constant initial piston speed should be changed to optimum, which is greater at low engine speeds - in terms of stroke. The Figure 3 presents this dependence together with other selected results of an engine with optimized mean piston speed, total turbocharger efficiency 60%, reference combustion duration 35 deg and bmep 30 bar. These features are a result of holistic approach to engine efficiency, which takes into account the conditions for boost pressure achievement.

Optimization does call for neither for rpm reduction nor for mean piston speed reduction, which might be slightly surprising. Even the optimum stroke is reached with higher mean piston speed than that of prototype engine. Despite very short burn duration and obvious mechanical efficiency increase (Figures 1 and 2) the bsfc at low speed is not too satisfying in comparison to medium speeds range.

The trend to long-stroke engine optimized for very low speed is changed at high speed due to the need of filling a cylinder via sufficiently large valves. The same trend features compression ratio, being optimized to lower values (and thus to lower temperatures at the end of compression) at low speed. These results are supported by found optimum valve timing, which prefers Miller-type cycle, while Atkinson one featured only small handicap if compared to Miller.

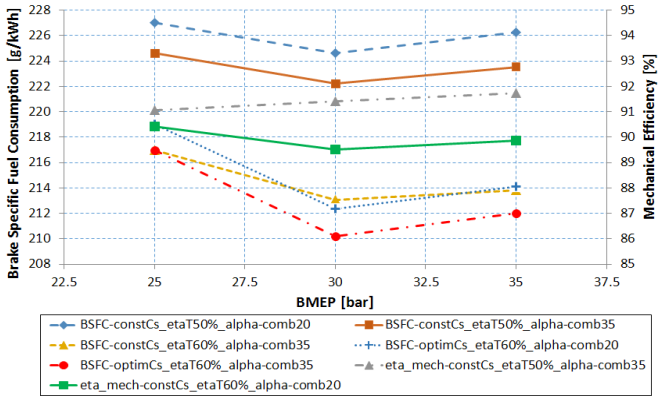

Figure 1. Optimization results – brake specific fuel consumption and mechanical efficiency as a function of engine load for engine speed 1 000 rpm and different engine optimization constraints (defined by constant or optimized mean piston speed, total turbocharger efficiency and combustion duration defined by the reference combustion angle).

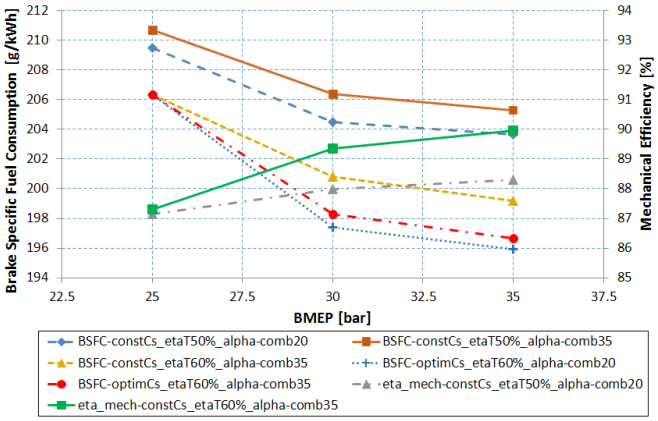

Figure 2. Optimization results – brake specific fuel consumption and mechanical efficiency as a function of engine load for engine speed 4 000 rpm and different engine optimization constraints (defined by constant or optimized mean piston speed, total turbocharger efficiency and combustion duration defined by the reference combustion angle).

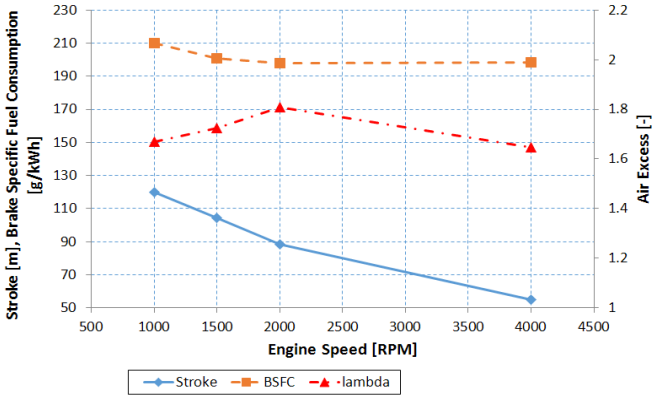

Figure 3. Optimization results – piston stroke, brake specific fuel consumption and air excess as a function of engine speed for engine with optimized mean piston speed, total turbocharger efficiency 60% and burn duration for the reference combustion angle 35 deg at bmep of 30 bar.

5. Engine Total Maps

After the WOT operation optimization, total maps of bsfc have been simulated for several selected variants of invariable values (stroke and compression ratio). Valve timing, combustion position and boost pressure (air excess with VN turbine) has been optimized continuously as it can be done at current engines, All maps are presented for torque, which makes easy comparison of differently downsized engines possible. The maps have been calculated for two variants of stroke, shorter for midspeed domain and longer stroke for downspeed use.

Obvious difference in minimum bsfc and slight improvement of low load range at the same torque due to continuous downsizing is visible in Figure 4 – Figure 8.

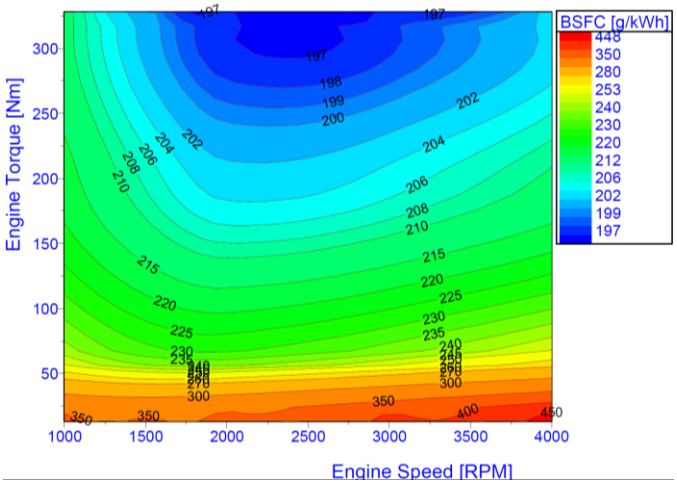

Figure 4. Map of brake specific fuel consumption as a function of engine speed and torque for engine with displacement 1.65 dm^3 (maximal bmep 25 bar) and stroke of 82 mm, total rated turbocharger efficiency 60% and reference combustion duration 35 deg CA.

As expected, long stroke is able to improve low speed range only with limited impact but it deteriorates higher speed range. It is necessary to simulate operation modes for the whole car before long stroke meaning is finally assessed.

The effect of longer stroke is evident for low speed end. Compression ratio has been kept on the high level of 18. Variable valve timing optimum tends to use Miller cycle even at low speed/load. Optimum air excess is comparatively low, as well. Those features are not very promising for fast transient load response since no margin of turbocharger speed or boost pressure is ensured at the start of load change. Advanced control system had to be developed before dynamic test procedures (especially ARTEMIS) are used for vehicle powertrain assessment. Before it, the mass and moments of inertia of downsized engines have to be estimated using parametric CAD controlled by DASY.

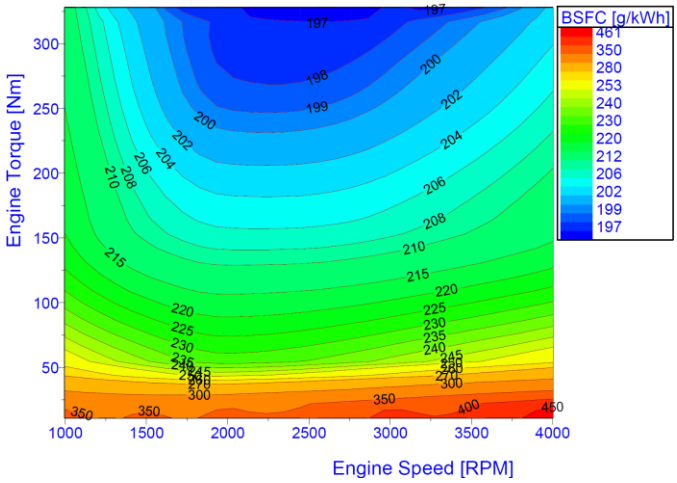

Figure 5. Map of brake specific fuel consumption as a function of engine speed and torque for engine with displacement 1.38 dm^3 (maximal bmep 30 bar) and stroke of 88.4 mm (compromising the whole speed range), total rated turbocharger efficiency 60% and reference combustion duration 35 deg CA.

6. Engine Design Changes during Downsizing

Crankshaft is a decisive component for bore spacing and engine mass if peak pressure is increased. Crankshaft dimensions for diesel engine were optimized to minimize crankshaft mass and cylinder block was designed roughly together with dimensions of a cylinder head to estimate engine weight for vehicle dynamic simulation - [17]. Minimum mass of engine is desired in real life, however. The masses of a cylinder block and a head have to be evaluated simultaneously with optimization, as well. The independent changes of different dimensions (bore spacing, height and width of a cylinder block or a cylinder head) pose some issues for very complicated shapes of those parts. From that reason, the simplified parametric CAD model was developed - [15].

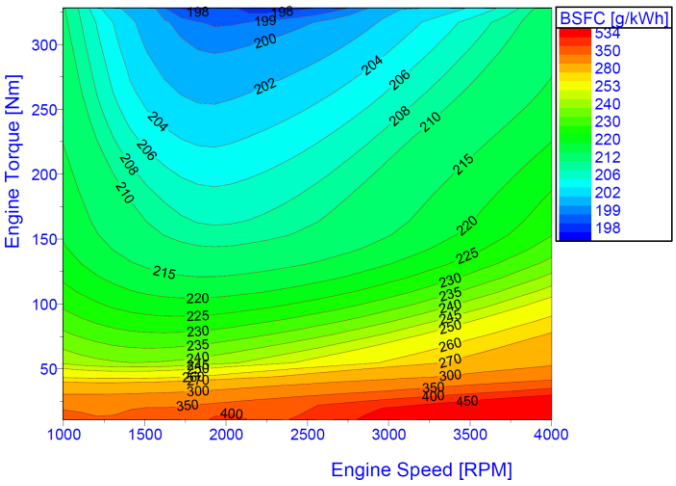

Figure 6. Map of brake specific fuel consumption as a function of engine speed and torque for engine with displacement 1.38 dm^3 (maximal bmep 30 bar) and stroke of 120 mm (optimum for a low speed range], total rated turbocharger efficiency 60% and reference combustion duration 35 deg CA.

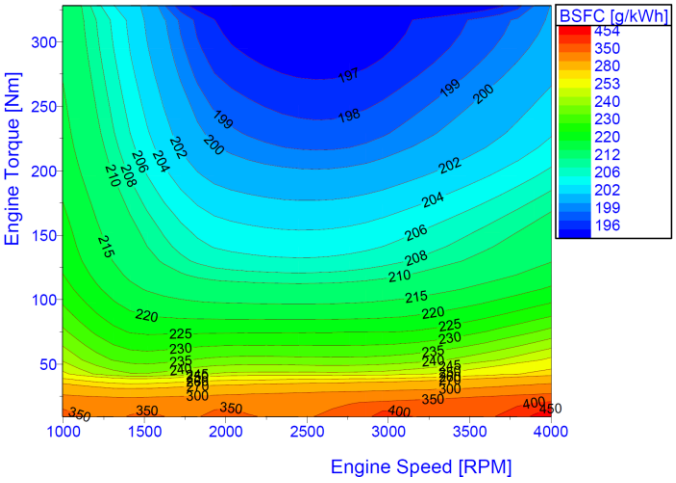

Figure 7. Map of brake specific fuel consumption as a function of engine speed and torque for engine with displacement 1.18 dm^3 (maximal bmep 35 bar) and stroke of 85 mm (compromising for the whole speed range), total rated turbocharger efficiency 60% and reference combustion duration 35 deg CA.

The main parts of a block (or a head) were split into two groups with wall thickness dependent on loads (typically cylinder wall thickness, main bearing supporting wall thickness, the walls or plates anchoring cylinder head or main bearing bolts, etc.) and load independent (all walls and covering decks sealing water or oil spaces, etc.). The wall thickness of a latter group is determined by manufacturing technology with the addition of mean thickness, calculated as mass equivalent of noise-avoiding ribs. Those thicknesses were applied separately (e.g., the bottom part of a crankcase) or just added to the thickness of loaded parts (e.g., the cylinder wall thickness). The representative thickness of unloaded walls may be found from existing design, including mass of ribs and cooling water, if necessary. The detail of DASY application have been published in [15] and [18].

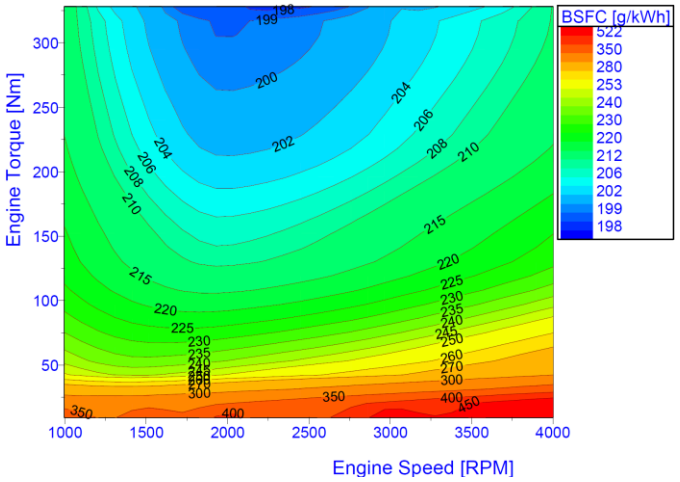

Figure 8. Map of brake specific fuel consumption as a function of engine speed and torque for engine with displacement 1.18dm^3 (maximal bmep 35 bar) and stroke of 115 mm low speed optimum), total rated turbocharger efficiency 60% and reference combustion duration 35 deg CA.

7. Engine Dynamic Features and Control

The simulations of load response are time consuming if simultaneous optimization is applied in the full 1-D model. The possibility to simplify the original model by procedures built in GT Power was used for this purpose. Nevertheless, fast running model (FRM) has been used with care and compared to the original full model in some extreme cases, especially for very high bmep. The general conclusion is there are only minor differences between both models but sometimes control stability problems may occur with FRM, perhaps due to longer integration step in comparison with the standard model. The slightly improved model of boost pressure controller had to be used since the level pulsation in turbine inlet is different in FRM.

The dynamic tests had to be done with the whole vehicle. The mass of downsized engines has been estimated by DASY using the procedures mentioned above and in [15]. Although the engine itself is significantly downsized, the rest of powertrain has to withstand the unchanged torque without changes in dimensions. Therefore, the mass of the powertrain is not changed too much. The gear stepping was kept without changes, however, slower engine speed was supported by transmission settings for longer stroke cases.

The car used for tests was a lower middle class one of the mass of 1 400 kg, equipped with 5 gear automatically shifted mechanical transmission. The possible changes of the car front end due to smaller engine, causing reduced mass and better drag resistance if downsized engine is used have not been taken into account yet.

The time of flexible acceleration at the fifth gear, starting from steady state with 50 km/h till 162 km/h (4000 rpm) is reached, has been chosen at this stage of investigation as an optimized parameter for control system development. No speed limit was set for the end of acceleration. The examples of car and engine parameters during this acceleration are presented in Figure 9 – Figure 11. The dynamic simulation had started for several seconds at low speed aiming at stabilized initial conditions. After this period, accelerator position was changed to WOT and the process of flexible acceleration was controlled using different strategies, based on look-up tables in the ECU, calibrated from steady operation optimization. Temporary mixture enrichment (air excess rack position) was allowed to accelerate the transient load response.

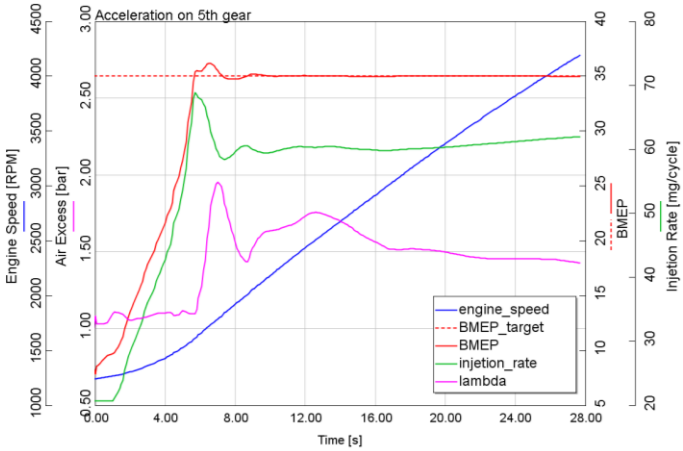

Figure 9. Flexible acceleration test of engine with maximum bmep 35 bar and stroke 115 mm on the 5th gear from 50 km/h – engine speed, net bmep, air excess and fuel injection rate controlled by lower limit of air excess (as presented in Figure 10)

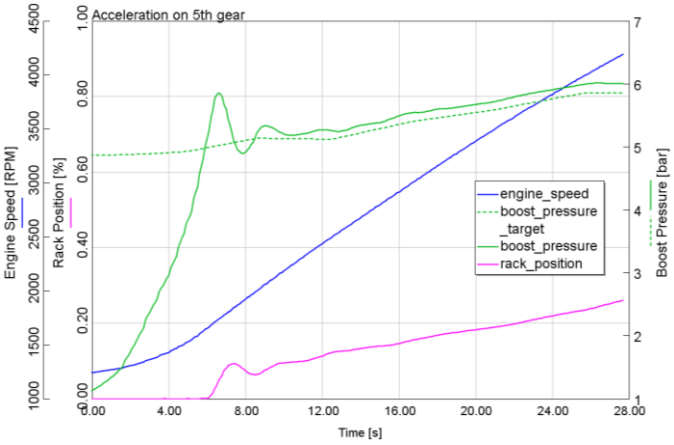

Figure 10. Flexible acceleration test of engine with maximum bmep 35 bar and stroke 115 mm on the 5th gear from 50 km/h – engine speed, net bmep, boost pressure and turbine rack position

As expected, the control using current speed/load bsfc optimized setting for steady operation reacted very slowly, especially due to Miller inlet valve timing and too opened variable nozzle turbine at the start of acceleration. The better results have been achieved using immediate switching to rack positions for intended target bmep, i.e., using accelerator position instead of the current fuelling of the engine. Turbine rack position was controlled to the desired values resulted from steady state optimizations. This control strategy has been tested later in fuel consumption tests. As expected, it is very fast but it is dependent on the result of steady state optimization where especially valvetrain timing is not the best for engine acceleration. As a compromise, the temporary switching to desired torque optimum parameters and turning back to optimized current engine state parameters proved to be the suitable solution, as well.

The results comparing different levels of downsizing/ downspeeding and control strategies are presented by a table in Figure 11.

time of acceleration [s]	bmep 25bar stroke 82mm	bmep 30bar stroke 88mm	bmep 30bar stroke 120mm	bmep 35bar stroke 85mm	bmep 35bar stroke 115mm
control strategies from steady states	23.7	26.8	25.8	28.7	25.9
temporary switching of control strategies	23.2	24.1	23.3	25.5	25.6

Figure 11. Time of flexible acceleration on the 5th gear using complete 1/D model for different downsizing levels with short and long stroke concepts and two control strategies approaches.

The results show increasing time for achieving the target speed if current state look/up table is applied. Applying control according reading of intended torque parameters (using accelerator position instead of current engine fueling signal) the times for acceleration are equal without influence of rated bmep or stroke. Higher desired boost pressure of more downsized engines resulted in worse acceleration times.

8. Driving Tests of Downsized Engines

After this analysis of control system, both standard NEDC and more dynamic ARTEMIS driving cycles were used for car economy assessment. As stated above, the impact of different engine mass on vehicle inertia was almost negligible, some influence of engine and turbocharger moments of inertia may be observed. It should be stressed once more here, that the engine parameters are estimates for yet non-existing downsized machines, yielding envelopes for real engine parameters only. Since the steady operation data are not very far from real-engine achieved results, there is hope that the dynamic response estimates are also rather realistic. The case of real two-stage turbocharger group reaction will be studied soon, nevertheless.

The NEDC pattern used for simulation, comparing engine and vehicle speed at fixed gear shifting, is

presented in Figure 12 (speeds) and in Figure 13 (engine torque, accelerator position and fuelling). Table of integral results of fuel consumption in both driving cycles is presented in Figure 15. The simulations were mostly done using full 1-D model to avoid any control issues and instabilities. Nevertheless, the FRM results are in close vicinity of them. Although the fuel economy results of current state control are quite promising, the dynamics of engine was completely unusable outside of "lazy" NEDC. Figure 14 presents the disadvantage of the control according to the current engine state parameters: the vehicle is not able to accelerate before the turbocharger reaches sufficient initial speed. The optimized valvetrain data for full load at steady state was too inappropriate for engine acceleration in this case.

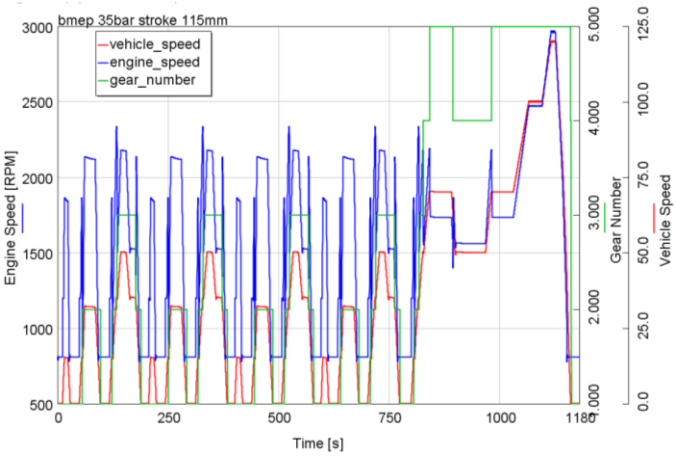

Figure 12. NEDC kinematic parameters of engine with maximum bmep 35 bar and stroke of 115 mm in simulation of NEDC.

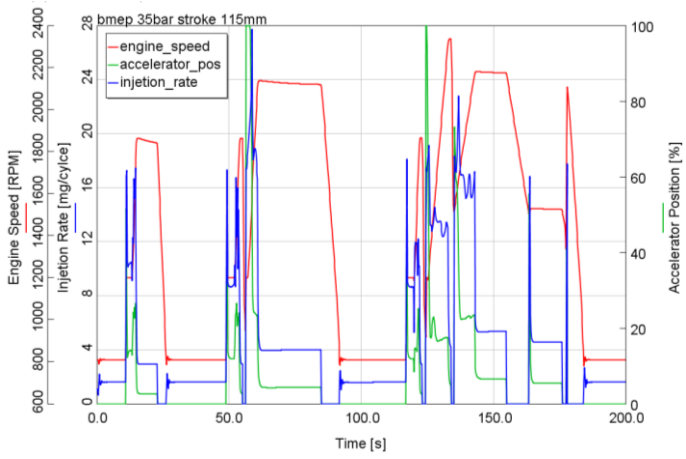

Figure 13. Engine parameters of engine with maximum bmep 35 bar and stroke of 115 mm in a part of simulation of NEDC.

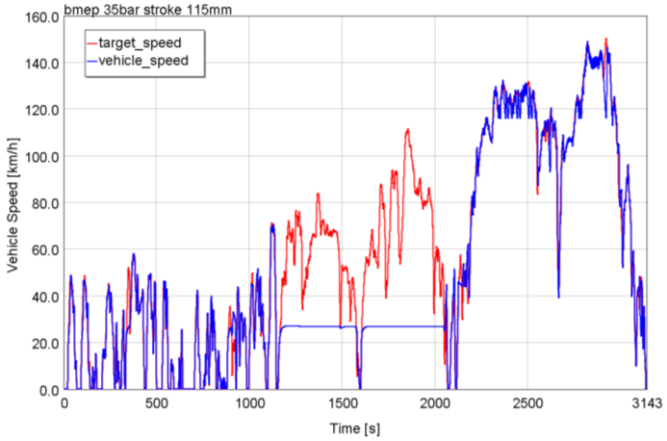

Figure 14. ARTEMIS required and achieved speed for engine control using current state parameters for engine with maximum bmep 35 bar and stroke of 115 mm.

No surprise that ARTEMIS cycle is much less economical than smooth, slow speed NEDC. This difference is followed in all cases of control and engine downsizing level. The advantage of downsizing is clearly demonstrated by the table in Figure 15 for any driving cycle and control strategy. More surprising is the absence of better results for downspeeded engines with optimized stroke, even if low transmission ratio powertrain is used. The reason is in much worse efficiency at higher speeds (see also Figure 3 and comparison, e.g., of Figure 7 and Figure 8).

Fuel consumption in driving cycle [l/100km]	bmep 25bar stroke 82mm		bmep 30bar stroke 88mm		bmep 30bar stroke 120mm		bmep 35bar stroke 85mm		bmep 35bar stroke 115mm	
	NEDC	ARTEMIS	NEDC	ARTEMIS	NEDC	ARTEMIS	NEDC	ARTEMIS	NEDC	ARTEMIS
Simple model based on fuel consumption maps	5.34	6.36	4.55	5.38	4.75	5.76	3.95	4.57	4.07	4.89
1/D engine model - control strategies from steady states	5.18	7.04	4.98	6.79	5.19	7.43	4.86	6.37	5.03	7.92
1/D engine model - temporary switching of control strategies	5.22	7.11	4.97	6.75	5.18	7.48	4.86	6.42	5.01	7.01
1/D engine model - temporary switching of control strategies and low ratios gearbox			4.74		4.80		4.55		4.66	
fuel consumption improvement for low ratio gearbox %			4.6		7.4		6.3		6.7	

Figure 15. Results of fuel consumption in NEDC and ARTEMIS cycles.

The application of target bmep control seems to be almost equivalent with switched target-current state control. Slow transient behavior of target bmep control can cause significant error in vehicle speed control leading in lower average speed and could cause lower fuel consumption. The driving cycle conditions are not met in those cases. Therefore, the temporary switching of control strategies is better even in NEDC. The fuel consumption is better especially in the cases of low transmission ratio powertrains, i.e., if engine is downspeeded. Nevertheless, even in this case the shorter stroke maps are better. The detailed explanation of those phenomena and more thoroughful optimization of unsteady operation has to be postponed for the near future.

9. Summary/Conclusions

The unconstrained thermodynamic optimization (no limits for peak pressure, fire surface or exhaust gas temperatures, very short optimized duration and position of combustion, reasonably matched turbocharger efficiency, etc.) does not call either for extreme peak pressures or very short combustion durations. The optimum air excess values reflect in-cylinder temperatures and speed. The optimum air excess decreases with increased engine speed, allowing for lower pumping losses. Their optimum values are suitable for advanced pollutant aftertreatment systems.

The results of unlimited optimization constraints have shown the importance of cooling loss at reduced engine speed and the need of a long-stroke engine design, if low speed is used dominantly in engine operation. Optimum valve timing requires a moderate Miller cycle, compression ratio being kept at standard values of 16-18, except for reduction at lowest speeds. It is caused again by the increase of cooling loss at low speed.

The current results demonstrated clearly that rightspeeding is very important. Downspeeding, reflected in lower cycle frequency (speed in rpm), positively increases time for unsteady events during combustion and gas exchange. Mechanical losses are reduced. However, the cycle cooling loss and the threat of knocking in the case of SI ICE are increased. According to the current results, a little more could be achieved if downspeeding in terms of mean piston speed is done only by moderate mean piston speed reduction. Long-stroke engines are worthwhile for low speed range only, nevertheless. If the engine is massively downsized and it uses the broad range of speed, long-stroke results in driving cycles are not better than those of standard engine dimensions.

Although there is only limited potential of further decreasing the total optimum of bsfc by massive downsizing in comparison to recent achievements, the car driving cycle results are still much better for downsized engines. The operation at partial loads and speeds achieves additional fuel savings in the case of car engines. This might not be so clear case for more loaded truck engines. The important general conditions for further reduction of fuel consumption can be achieved by increasing turbocharger efficiency (accompanied by the reduction of pressure losses in pipe systems), keeping minimum necessary air excess for combustion and pollutants. Surprisingly, the duration of combustion is not critical for the current combustion systems with already fast combustion. More might be achieved if **unsteady** heat transfer to cooled walls is limited. This remains as a challenge for the future.

The comparison with envelope of achievable efficiencies and dimensions has demonstrated the yet unused potential of fully flexible engine. The further works are being already focused on assessment of low speed/load operation of engines and their dynamic response, including smart control systems and combined turbo-supercharging. Both of these features are unavoidable for vehicle road test application. The results of dynamic response simulations may employ even 3-D models, as demonstrated, e.g., in [11]. The specific cases of SI engines and two-stroke charge exchange are being investigated separately, using the results of this study in appropriate way.

Considering future ICE improvement, the relevance of correctly simulated model of wall heat transfer inside a cylinder calls for further experimental investigation of this issue together with assessment of wall insulation by low thermal inertia materials. The second decisive factor is turbocharger or supercharger efficiency improvement. The future research will be focused on coupling waste-heat recovery cycles to current ICE performance considering the size and weight of appropriate systems with impacts to vehicle performance, which is possible in DASY. The overall goal – finding the best solution for future cars with reasonable range and environment friendly features – calls for this holistic approach used, as well, for future battery vehicles.

10. Acknowledgments

This work was supported by:

- Technological Agency, Czech Republic, programme Centre of Competence, project #TE01020020 Josef Božek Competence Centre for Automotive Industry.
- EU Regional Development Fund in OP R&D for Innovations (OP VaVpI) and Ministry of Education, Czech Republic, project #CZ.1.05/2.1.00/03.0125 Acquisition of Technology for Vehicle Center of Sustainable Mobility.
- The Grant Agency of the Czech Technical University in Prague, grant No. SGS13/184/OHK2/3T/12.

This support is gratefully acknowledged.

11. References

1. Eilts, P. et al.: Investigation of Extreme Mean Effective and Maximum Cylinder Pressures in a Passenger Car Diesel Engine. SAE Paper 2013-012-1622

2. Hyvonen J.: Higher Efficiency for Further Downsizing; Example from Large Bore Medium Speed Engines (Wärtsilä). High Efficiency IC Engine Symposium, SAE 2013
3. Curtis E.: Near Term Combustion System Development and the Influence of Transmissions, Drive Cycles and Fuels (Ford Motor Company). High Efficiency IC Engine Symposium, SAE 2013
4. Reitz R.: Reactivity Controlled Compression Ignition (RCCI) for Ultra-High Efficiency IC Engine Operation with Low NOx and PM Emissions Plus Transient Control. High Efficiency IC Engine Symposium, SAE 2013
5. Bogomolov S., Mikulec A., Macek J. (2011). Development of Design Assistance System and Its Application for Engine Concept Modeling, SAE Technical Paper 2011-37-0030, 2011, *SAE World Congress 2011*, doi: 10.4271/2011-37-0030
6. Hejlsberg A., Torgersen M., Wiltamuth S., Golde P. (2010). C# Programming Language, The (4th Edition)
7. Mifa Kim, Tomoyuki Hiroyasu, Mitsunori Miki, Shinya Watanabe (2004). SPEA2+: Improving the Performance of the Strength Pareto Evolutionary Algorithm 2, *Parallel Problem Solving from Nature – PPSN VIII, 8th International Conference*, Proceedings pp 742-751.
8. Bogomolov S., Mikulec A., Macek J., Valasek M., Doleček V. (2012). Knowledge-Based Design and Optimization of Engines, *THIESEL 2012 Conference on Thermo- and Fluid Dynamic Processes in Direct Injection Engines*.
9. Emrich M., Fuente D.S.J., Macek J.: Simple Physical Model of ICE Mechanical Losses. SAE Paper 2011-01-0610
10. Vítek, O., Macek, J., Polášek, M.: New Approach to Turbocharger Optimization using 1-D Simulation Tools. SAE Paper 2006-01-0438
11. Macek J., Vítek O., Doleček V., Srinivasan S., Tanner F.X.: Optimization of Engine Control Strategies during Transient Processes Combining 1-D and 3-D Approaches. SAE Paper 2010-01-0783
12. Heywood J.B.: Internal Combustion Engine Fundamentals. McGraw Hill 1998
13. Macek J.: Optimization of Using Fuel Chemical Energy in Reciprocating Engines. Doctor of Science Dissertation, Czech Technical University 1989, 631 pp.
14. Macek J., Foglar P., Holmberg S.: The Development of Working Cycle and Design of a Four-Stroke, Medium Speed, Heavy Fuel Engine of 275 mm Bore. CIMAC Paper, Oslo 1985
15. Bogomolov, S., Dolecek, V., Macek, J., Mikulec, A, Vitek O. "Combining Thermodynamics and Design Optimization for Finding ICE Downsizing Limits," SAE Technical Paper 2014-01-1098, 2014, doi:10.4271/2014-01-1098.
16. Vítek O., Macek J., Doleček V., Bogomolov S., Mikulec A., Barák A.: Realistic Limits Of Ice Efficiency. FISITA Paper F2014-CET-051
17. Bogomolov S., Macek J., Mikulec A., Novotny T., Kazda J.: Early Stage Optimization of Crankshaft Mass Using Design Assistance System (DASY). FISITA Paper F2014-LWS-024
18. Bogomolov S., Macek J., Mikulec A., Dolecek V., Valasek M.: Early-stage assessment of innovations for vehicle powertrains using Design Assistance System. Transport Research Arena EU, Paris 2014

12. Definitions/Abbreviations

bmep	brake mean effective pressure
bsfc	brake specific fuel consumption
CA	crank angle
CI	compression ignition
CR	compression ratio
c s, c_s	mean piston speed
D	diameter, cylinder bore
DASY	design assistance system
delta alpha s	combustion duration (0-95% fuel burnt) in CA
eta mech	mechanical efficiency of an engine
eta T	total turbocharger efficiency (virtual turbocharger surrogates the real two-stage turbocharging)
FEM	finite element method
FIE	fuel injection equipment
FMEP	friction mean effective pressure
HCCI	homogeneous charge compression ignition
ICE	internal combustion engine
lambda	air excess (relative air-to-fuel ratio)
NOx	sum of polluting nitrogen oxides
NVH	noise, vibration and harshness
n	engine speed (rpm)
PCCI	premixed charge compression ignition
PID	proportional-derivative-integrating controller
P_e	brake power
p_e	brake mean effective pressure
p_{im}	boost pressure
p_{max}, p max	cylinder peak pressure
PM	particulate matter (exhaust pollutant)
RB	connecting rod bearing
RBL	connecting rod bearing journal length
RCCI	reaction controlled compression ignition
SCR	selective catalytic reduction of NOx

SI	spark ignition	**WOT**	wide-opened throttle
VNT	variable nozzle turbine		

13. Appendix

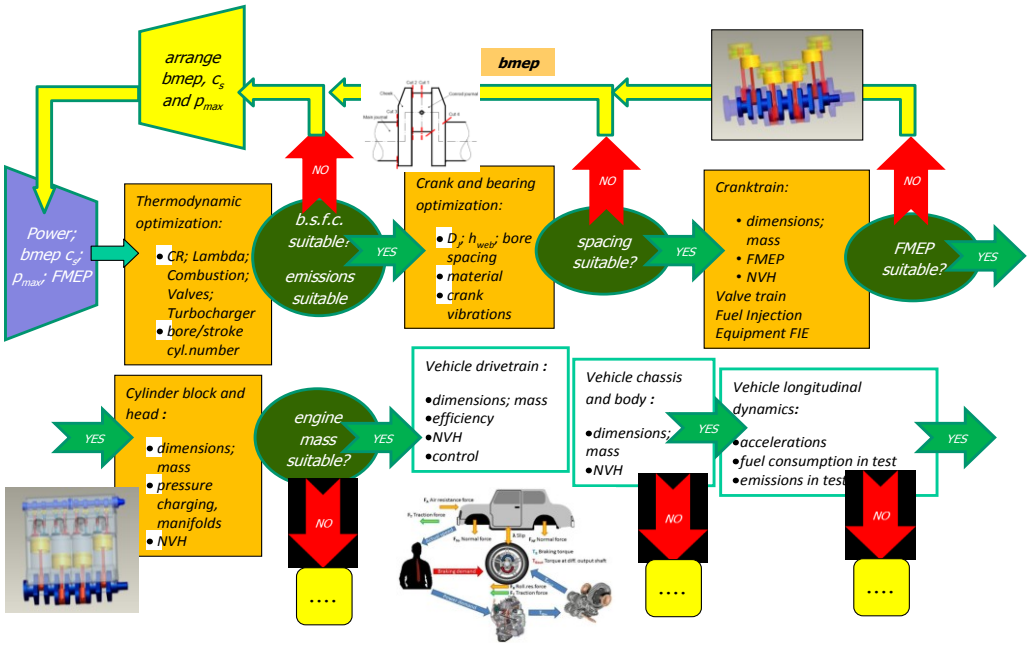

Figure 16. Data flows during coupled thermodynamic and design optimization.